Hence from (38)

$$E\{h_{z,\theta}(p'_\beta(t+1))/\mathbb{P}(t)\} \leqslant h_{z,\theta}(p'_\beta(t)),$$

for all t and $\mathbb{P}(t)$. (53)

Q.E.D.

Proof of Theorem 2: From Lemma 2 and Lemma 4 we can prove $\lim_{\theta\to 0}\lim_{t\to\infty} E\{p_\beta(t)\} = 1$ (see [3], [7]). This means that the GL_{R-I} scheme is ϵ-optimal in the general n-teacher environment satisfying (7). Q.E.D.

Acknowledgment

The author would like to thank Prof. Y. Sawaragi (Kyoto Sangyo Univ., Japan), Prof. T. Soeda (Tokushima Univ., Japan), Prof. T. Shoman (Tokushima Univ.), Prof. J. Carter (Tokushima Univ.), and Mr. K. Shimotake (Tokushima Univ.) for their kind assistance.

References

[1] V. I. Varshavskii and I. P. Vorontsova, "On the behavior of stochastic automata with variable structure," *Automat. Remote Contr.*, vol. 24, pp. 353-360, 1963.

[2] B. Chandrasekaran and D. W. C. Shen, "On expediency and convergence in variable-structure automata," *IEEE Trans. Syst., Sci., Cybern.*, vol. SSC-4, pp. 52-60, Mar. 1968.

[3] M. F. Norman, "On linear models with two absorbing barriers," *J. Math. Psychology*, vol. 5, pp. 225-241, 1968.

[4] I. J. Shapiro and K. S. Narendra, "Use of stochastic automata for parameter self-optimization with multimodal performance criteria," *IEEE Trans. Syst., Sci., Cybern.*, vol. SSC-5, pp. 352-360, Oct. 1969.

[5] K. S. Fu, "Stochastic automata as models of learning systems," in *Adaptive, Learning, and Pattern Recognition Systems: Theory and Applications*, J. M. Mendel and K. S. Fu, Eds. New York: Academic, 1970, pp. 393-431.

[6] S. Lakshmivarahan and M. A. L. Thathachar, "Absolutely expedient learning algorithms for stochastic automata," *IEEE Trans. Syst., Man, Cybern.*, vol. SMC-3, pp. 281-286, May 1973.

[7] Y. Sawaragi and N. Baba, "Two ϵ-optimal nonlinear reinforcement schemes for stochastic automata," *IEEE Trans. Syst., Man, Cybern.*, vol. SMC-4, no. 1, pp. 126-131, Jan. 1974.

[8] S. Lakshmivarahan and M. A. L. Thathachar, "Bounds on the probability of convergence of learning automata," Tech. Rep., Indian Institute of Science, Bangalore, India, 1974.

[9] K. S. Narendra and M. A. L. Thathachar, "Learning automata—A survey," *IEEE Trans. Syst., Man, Cybern.*, vol. SMC-4, pp. 323-334, July 1974.

[10] N. Baba and Y. Sawaragi, "On the learning behavior of stochastic automata under a nonstationary random environment," *IEEE Trans. Syst., Man, Cybern.*, vol. SMC-5, no. 3, pp. 273-275, Mar., 1975.

[11] D. E. Koditschek and K. S. Narendra, "Fixed structure automata in a multi-teacher environment," *IEEE Trans. Syst., Man, Cybern.*, vol. SMC-7, pp. 616-624, Aug. 1977.

[12] K. S. Narendra and S. Lakshmivarahan, "Learning automata-A critique," Tech. Rep. 7703, Yale University, New Haven, CT, 1977.

[13] Y. M. El-Fattah, "Stochastic automata modeling of certain problems of collective behavior," *IEEE Trans. Syst., Man, Cybern.*, vol. SMC-10, pp. 304-314, June 1980.

[14] J. L. Doob, *Stochastic Processes*. New York: Wiley, 1953.

[15] M. F. Norman, *Markov Processes and Learning Models*. New York: Academic, 1972.

Histogram Concavity Analysis as an Aid in Threshold Selection

AZRIEL ROSENFELD, FELLOW, IEEE, AND PILAR DE LA TORRE

***Abstract*—A well-known heuristic for segmenting an image into gray level subpopulations is to select thresholds at the bottoms of valleys on the image's histogram. When the subpopulations overlap, valleys may not exist, but it is often still possible to define good thresholds at the "shoulders" of histogram peaks. Both valleys and shoulders correspond to concavities on the histogram, and this suggests that it should be possible to find good candidate thresholds by analyzing the histogram's concavity structure. Histogram concavity analysis as an approach to threshold selection is investigated and its performance on a set of histograms of infrared images of tanks is illustrated.**

Manuscript received September 1, 1981; revised September 7, 1982. This work was supported by the National Science Foundation under Grant MCS-79-23422.

The authors are with the Computer Vision Laboratory, Computer Science Center, University of Maryland, College Park, MD 20742

I. Introduction

Many types of images contain objects that occupy a different range of gray levels than their background. Such images can be segmented by gray level thresholding to separate the object and background ranges. If these ranges are sufficiently separated, the object and background subpopulations give rise to distinct peaks on the image's histogram, and a good threshold can usually be selected at the bottom of the valley between these peaks [1], [2]. If the ranges overlap there may be no valley, but there may be a "shoulder" on the background peak where the object peak overlaps it, and it is often still possible to pick a good threshold at the "root" of this shoulder. For a survey of threshold selection techniques see [3].

Identification of valleys and shoulders on a histogram is itself a nontrival problem. Histograms are usually "noisy" and contain many valleys defined by noise spikes. What one really wants is "significant" valleys, in terms of the heights (or areas) of the neighboring peaks and the depth (or area) of the valley itself. However, the extents of peaks and valleys are themselves not easy to define. (It would be of interest to apply methods of hierarchical waveform analysis [4]–[6] to determining significant peaks and valleys in a histogram, but this does not seem to have as yet been attempted.) Defining "significant" shoulders is at least equally difficult.

Both valleys and shoulders correspond to concavities on the histogram, and this suggests that it should be possible to find good candidate thresholds by analyzing the histogram's concavity structure. This note investigates histogram concavity analysis as an approach to threshold selection, and illustrates its performance on a set of histograms of infrared images of tanks (Figs. 1–7).

II. Histogram Concavities

Let the given histogram H be defined over the set of gray levels $K, \cdots, L$, and have bar heights $h(H), \cdots, h(L)$, where $h(K)$ and $h(L)$ are nonzero, and all the h's are nonnegative. We shall regard H as a two-dimensional region bounded on the left, bottom, and right by the straight lines $\overline{(K,0)(K,h(K))}$, $\overline{(K,0)(L,0)}$, and $\overline{(L,0)(L,h(L))}$, respectively (Fig. 8).

To find the concavities of H we construct its convex hull; this is the smallest convex polygon $\overline{H}$ containing H, and the concavities are found by taking the set-theoretic difference $\overline{H} - H$. (A concavity can be defined as a connected component of $\overline{H} - H$.) It is easily seen that the three straight lines that bound H on the left, right, and bottom are sides of $\overline{H}$; thus we only need to construct the part of $\overline{H}$ defined by the tops of the histogram bars.

A simple algorithm for constructing $\overline{H}$ by a left-to-right scan of H is as follows [7]. Starting at $(K, h(K))$, compute the slopes θ_i of the line segments $\overline{(K,h(K))(i,h(i))}$, $K+1 \leqslant i \leqslant L$, where $-90° < \theta_i < 90°$. Let θ_{K_1} be the largest of these slopes, and let K_1 be the rightmost point having this slope. Then $\overline{(K,h(K))(K_1,h(K_1))}$ is a side of the convex hull (see Fig. 7). We now repeat the process with K_1 replacing K, i.e., we compute the slopes of the segments $(K_1, h(K_1))(i, h(i))$, $K_1 + 1 \leqslant i \leqslant L$, find the largest slope θ_{K_2} and the rightmost point K_2 having this slope, yielding $\overline{(K_1,h(K_1))(K_2,h(K_2))}$ as a side of the convex hull, and so on, until we reach L.

0018-9472/83/0300-0231$01.00 ©1983 IEEE

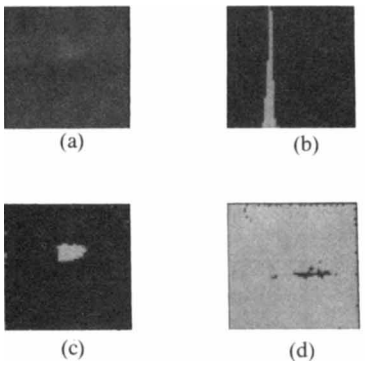

Fig. 1. Test image. (a) Image. (b) Histogram. (c) and (d) Thresholded images.

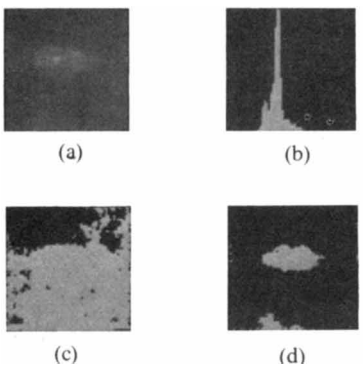

Fig. 2. Test image. (a) Image. (b) Histogram. (c) and (d) Thresholded images.

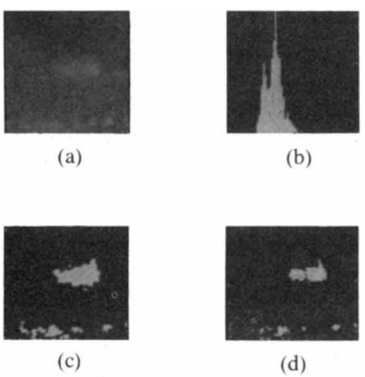

Fig. 3. Test image. (a) Image. (b) Histogram. (c) and (d) Thresholded images.

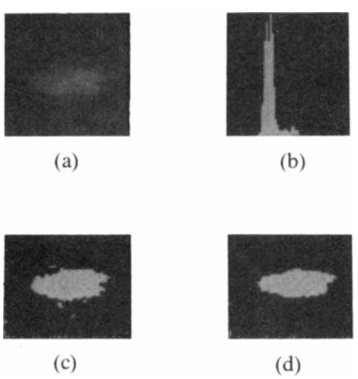

Fig. 4. Test image. (a) Image. (b) Histogram. (c) and (d) Thresholded images.

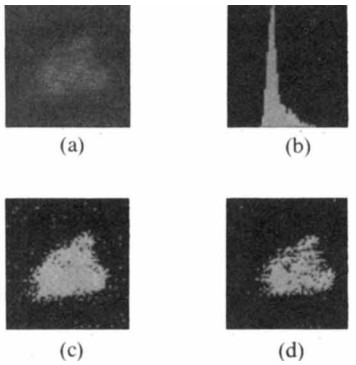

Fig. 5. Test image. (a) Image. (b) Histogram. (c) and (d) Thresholded images.

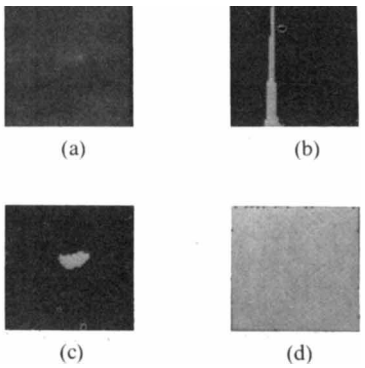

Fig. 6. Test image. (a) Image. (b) Histogram. (c) and (d) Thresholded images.

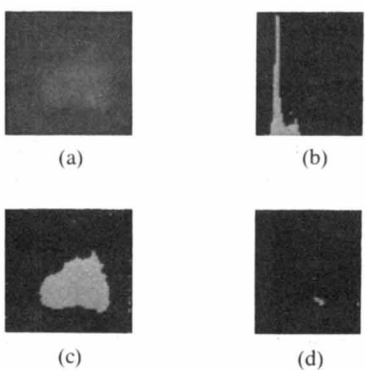

Fig. 7. Test image. (a) Image. (b) Histogram. (c) and (d) Thresholded images.

Fig. 8. Histogram regarded as two-dimensional region.

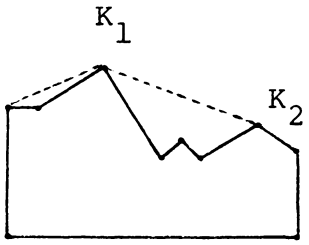

Fig. 9. Convex hull construction.

Whenever H lies strictly below $\bar{H}$ we have a concavity in H. Note that concavities can themselves have a complex structure of "subconcavities" (see the simple example in Fig. 9 between K_1 and K_2). One could construct a hierarchical representation of this concavity structure (e.g., [8], [9]), but this was not felt to be necessary for our application. Note also that the concavity associated with a valley does not exactly coincide with the intuitive definition of the valley; the corresponding side of $\bar{H}$ does not touch H at the maxima of the peaks bordering the valley, but rather at "inflection" points along the sides of the peaks where they change from being convex to being concave.

III. Using Deepest Concavity Points as Thresholds

Any concavity in the histogram is a possible location for a threshold, but not all points of the concavity are equally good candidates. Let $\bar{h}(i)$ be the height of $\bar{H}$ at gray level i. Thus $\bar{h}(i) - h(i)$ is the vertical distance between the top of the histogram bar $h(i)$ and the border of $\bar{H}$. We shall consider as candidates for threshold positions those points i for which $\bar{h}(i) - h(i)$ is a local maximum; these are the (vertically) deepest concavity points. Note that if i is not in a concavity we have $\bar{h}(i) = h(i)$, so that their difference is zero.

To illustrate this idea let us examine a set of examples involving infrared images of tanks. Figs. 1–7 show the images (upper left) and their histograms (upper right). These histograms have large peaks (sometimes split into two parts) representing the background, and small peaks or shoulders representing the tanks. The histogram bar heights $h(i)$ are tabulated in the second columns of Tables I–VII, and the vertical distances $\bar{h}(i) + h(i)$ in the third columns. We see that the functions $\bar{h}(i) - h(i)$ do have fewer maxima than the histograms themselves.

Not all of these maxima, however, are equally good candidates for threshold selection. In some of the histograms (cf. Figs. 4, 6, 7) a large concavity is produced by a single noise point lying far to the left of the main body of the histogram. If this point were removed, the leftmost K for which $h(K) > 0$ would change substantially, and this concavity would be greatly reduced or eliminated. Thus we see that the histogram concavity structure is quite sensitive to noise of this type (small numbers of nonzero values outside the main gray level range). Of course, noise can also change the structure in other ways (e.g., a concavity can split into two parts if a histogram peak just touches a side of $\bar{H}$), but such changes do not greatly affect the locations of the deepest concavity points. The principal problem caused by noise is the creation of "spurious concavities" outside the main part of the histogram.

IV. Coping with Spurious Concavities

One way to reduce the effects of noise is to smooth the histogram before constructing its convex hull. However, if we want to eliminate spurious concavities completely, we must completely remove the noise points which give rise to them, and this entails making a decision as to whether a given set of isolated nonzero h values is noise or represents a significant subpopulation of pixels. We can avoid the need for such decisions by allowing the spurious concavities to remain, but computing a figure of merit with respect to which they evaluate very poorly.

TABLE I

Gray Level (i)	Histogram value (h(i))	Depth of concavity $(\bar{h}-h)\times10^{-2}$	$E\times10^{-5}$
13	1	0.00	0.00
14	2	1.70	0.04
15	2	3.41	0.12
16	7	5.07	0.20
17	65	6.20	0.49
18	300	5.56	3.09
19	671	3.56	14.02
20	1198	0.00	31.94
21	1155	0.00	41.55
22	480	5.47	23.64
23	98	8.01	8.34
24	32	7.38	4.66
25	27	6.15	3.41
26	18	4.96	2.34
27	13	3.73	1.62
28	13	2.44	1.10
29	13	1.16	0.57
30	1	0.00	0.04

TABLE II

Gray Level (i)	Histogram value (h(i))	Depth of concavity $(\bar{h}-h)\times10^{-2}$	$E\times10^{-5}$
13	1	0.00	0.00
14	6	0.59	0.04
15	13	1.16	0.29
16	37	1.56	0.82
17	144	1.13	2.30
18	179	1.42	7.83
19	172	2.12	14.12
20	122	3.26	19.56
21	225	2.87	23.06
22	284	2.92	28.74
23	600	0.40	34.46
24	704	0.00	41.24
25	696	0.00	40.02
26	313	3.59	29.06
27	131	5.17	20.98
28	75	5.49	17.01
29	67	5.33	14.59
30	69	5.07	12.32
31	47	5.05	9.90
32	42	4.86	8.20
33	47	4.57	6.64
34	27	4.53	4.85
35	30	4.26	3.80
36	27	4.05	2.62
37	13	3.95	1.54
38	9	3.75	1.02
39	1	3.59	0.65
40	1	3.36	0.61
41	3	3.10	0.57
42	1	2.88	0.45
43	3	2.62	0.41
44	3	2.38	0.29
45	0	2.17	0.16
46	2	1.91	0.16
47	0	1.69	0.08
48	0	1.45	0.08
49	0	1.21	0.08
50	0	0.97	0.08
51	0	0.73	0.08
52	0	0.49	0.08
53	1	0.24	0.08
54	1	0.00	0.04

A spurious concavity is characterized by the fact that nearly all of the histogram lies on one side of it, and almost none on the other side. Suppose that for every i we compute $E_i \equiv (\sum_{j=K}^{i-1} h(j))(\sum_{j=i}^{L} h(j))$. This quantity is zero when $i = K$ or L, and is a maximum when i is at the median of the histogram (equal areas on both sides of it), so that it measures the "balance" of the histogram around the value i. The fourth column of Tables I–VII shows the values of E_i for each i for the seven histograms. As expected, these measures are quite low for points in the spurious concavities. Thus one can eliminate spurious concavities by ignoring maxima of $\bar{h} - h$ for which E is very small.

V. Evaluating Concavity Points as Thresholds

If one has *a priori* knowledge about the desired segmentation (e.g., the relative areas of objects and background are approximately known), one should use this knowledge in choosing among the maxima. For example, in the case of Figs. 1–7, we know that the tanks are brighter than the background. Figs. 1–7 (bottom)

TABLE III

Gray Level (i)	Histogram value (h(i))	Depth of concavity $(\bar{h}-h)\times10^{-2}$	$E\times10^{-5}$
12	1	0.00	0.00
13	8	0.55	0.04
14	52	0.74	0.37
15	87	1.01	2.46
16	212	0.39	5.84
17	313	0.00	13.45
18	256	0.95	23.04
19	201	1.88	29.42
20	210	2.17	33.52
21	334	1.31	36.93
22	414	0.89	40.54
23	541	0.00	41.93
24	351	1.62	38.57
25	331	1.53	33.26
26	218	2.38	25.99
27	161	2.66	20.01
28	73	3.26	14.98
29	100	2.70	12.53
30	61	2.81	9.00
31	59	2.55	6.75
32	36	2.49	4.50
33	31	2.26	3.09
34	16	2.12	1.86
35	5	1.95	1.22
36	14	1.58	1.02
37	4	1.39	0.45
38	2	1.13	0.29
39	3	0.83	0.20
40	1	0.57	0.08
41	0	0.29	0.04
42	1	0.00	0.04

TABLE IV

Gray level (i)	Histogram value (h(i))	Depth of concavity $(\bar{h}-h)\times10^{-2}$	$E\times10^{-5}$
2	1	0.00	0.00
3	0	0.39	0.04
4	0	0.76	0.04
5	0	1.14	0.04
6	0	1.52	0.04
7	0	1.90	0.04
8	0	2.27	0.04
9	0	2.65	0.04
10	0	3.03	0.04
11	0	3.40	0.04
12	0	3.78	0.04
13	1	4.15	0.04
14	1	4.52	0.08
15	16	4.75	0.12
16	27	5.02	0.77
17	185	3.82	1.86
18	535	0.69	8.93
19	642	0.00	25.51
20	530	1.29	37.85
21	675	0.00	41.82
22	575	0.71	38.75
23	277	3.39	28.95
24	96	4.91	21.86
25	69	4.89	19.05
26	39	4.90	16.92
27	41	4.58	15.67
28	33	4.37	14.32
29	50	3.91	13.21
30	40	3.72	11.49
31	27	3.55	10.08
32	59	2.94	9.11
33	61	2.63	6.94
34	34	2.61	4.62
35	32	2.33	3.29
36	20	2.16	2.02
37	5	2.02	1.22
38	7	1.71	1.02
39	6	1.42	0.73
40	7	1.12	0.49
41	1	0.89	0.20
42	2	0.59	0.16
43	0	0.31	0.08
44	2	0.00	0.08

show the results of thresholding the images at the two maxima of $\bar{h}-h$ that have the brightest gray levels. We see that at least one of these extracts the tank in all cases.

Alternatively, given a criterion for evaluating the goodness of a segmentation (e.g., low "busyness" of the thresholded image [10], or a good match between the borders of above-threshold regions

TABLE V

Gray level (i)	Histogram value (h(i))	Depth of concavity $(\bar{h}-h)\times10^{-2}$	$E\times10^{-5}$
14	7	0.00	0.00
15	12	0.94	0.29
16	58	1.48	0.77
17	188	1.17	3.09
18	366	0.39	10.15
19	504	0.00	21.86
20	579	0.00	33.61
21	592	0.00	40.83
22	382	1.90	41.28
23	264	2.87	37.85
24	158	3.73	33.77
25	112	3.98	30.66
26	119	3.71	28.16
27	103	3.67	25.22
28	72	3.77	22.45
29	97	3.32	20.39
30	87	3.22	17.45
31	70	3.18	14.65
32	66	3.02	12.29
33	53	2.94	9.97
34	40	2.87	8.05
35	27	2.80	6.56
36	28	2.58	5.54
37	22	2.44	4.46
38	19	2.27	3.61
39	10	2.15	2.86
40	12	1.93	2.46
41	12	1.72	1.98
42	15	1.49	1.50
43	5	1.39	0.90
44	8	1.15	0.69
45	2	1.01	0.37
46	2	0.81	0.29
47	2	0.60	0.20
48	2	0.40	0.12
49	0	0.21	0.04
50	1	0.00	0.04

TABLE VI

Gray level (i)	Histogram value (h(i))	Depth of concavity $(\bar{h}-h)\times10^{-2}$	$E\times10^{-5}$
2	1	0.00	0.00
3	0	0.60	0.04
4	0	1.19	0.04
5	0	1.78	0.04
6	0	2.37	0.04
7	0	2.95	0.04
8	0	3.54	0.04
9	0	4.13	0.04
10	0	4.72	0.04
11	0	5.31	0.04
12	0	5.90	0.04
13	0	6.49	0.04
14	1	7.07	0.04
15	2	7.65	0.08
16	11	8.14	0.16
17	80	8.04	0.61
18	427	5.16	3.80
19	811	1.91	18.66
20	1061	0.00	36.83
21	1094	0.00	40.75
22	407	5.07	21.21
23	99	6.35	7.83
24	50	5.04	4.07
25	19	3.54	2.10
26	20	1.73	1.34
27	13	0.00	0.53

and the maxima of the gray level gradient [11]), one can test all the thresholds defined by the maxima of $\bar{h}-h$, and choose the one for which the thresholded image has the highest evaluation. Since there are usually very few maxima, this should be computationally inexpensive.

The maxima of $\bar{h}-h$ are generally reasonable locations for thresholds, but they may not always be optimal. If a concavity is bounded by two peaks of approximately equal height (i.e., $h(K_j) \approx h(K_{j+1})$), the maximum of $\bar{h}-h$ in this concavity will be approximately at the lowest point of the valley. However, if the peak heights are very unequal (or in the case of a shoulder), e.g., $h(K_j) \gg h(K_{j+1})$, the maximum will usually be close to the higher peak, where h is dropping faster than $\bar{h}$ (see Fig. 10). This suggests that we should regard the maxima of $\bar{h}-h$ as tentative threshold locations, and should evaluate other thresholds near these maxima to see whether improvements can be obtained.

TABLE VII

Gray level (i)	Histogram value (h(i))	Depth of concavity $(\bar{h}-h)\times10^{-2}$	$E\times10^{-5}$
0	1	0.00	0.00
1	0	0.45	0.04
2	0	0.90	0.04
3	0	1.34	0.04
4	0	1.79	0.04
5	0	2.23	0.04
6	0	2.67	0.04
7	0	3.12	0.04
8	0	3.56	0.04
9	0	4.01	0.04
10	0	4.45	0.04
11	6	4.83	0.04
12	4	5.30	0.29
13	5	5.73	0.45
14	8	6.15	0.65
15	15	6.52	0.98
16	8	7.04	1.58
17	16	7.40	1.90
18	14	7.86	2.54
19	20	8.25	3.09
20	116	7.73	3.88
21	579	3.55	8.27
22	978	0.00	26.17
23	950	0.00	41.17
24	320	5.71	37.43
25	187	6.45	32.10
26	109	6.64	28.04
27	91	6.22	25.35
28	81	5.73	22.93
29	102	4.93	20.63
30	106	4.30	17.54
31	98	3.79	14.12
32	141	2.77	10.76
33	95	2.64	5.58
34	31	2.69	1.86
35	7	2.34	0.61
36	2	1.79	0.33
37	0	1.22	0.25
38	2	0.61	0.25
39	4	0.00	0.16

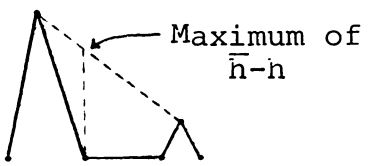

Fig. 10. Maxima of $\bar{h}-h$ tend to lie near high peaks.

Again, this is computationally reasonable, since there are normally only a few maxima.

VI. Concluding Remarks

Histogram valleys and shoulders, which are usually good locations for thresholds, are associated with concavities on the histogram. This suggests that concavity points of maximum "depth" are good candidates for thresholds. These points can be located efficiently by constructing the convex hull of the histogram. Since normally there are very few of them, they can be individually evaluated (or we can even evaluate sets of thresholds in their vicinities) in terms of the quality of the resulting segmentation. This concavity analysis of the histogram provides a useful approach to reducing the amount of information that must be processed in order to identify good thresholds.

Acknowledgment

The help of D. Lloyd Chesley in preparing this paper is gratefully acknowledged.

References

[1] J. M. S. Prewitt and M. Mendelsohn, "The analysis of cell images," *Ann. N.Y. Acad. Sci.*, vol. 128, pp. 1035–1053, 1966.
[2] A. Rosenfeld and A. C. Kak, *Digital Picture Processing*. New York: Academic, 1976, Section 8.1.
[3] J. S. Weszka, "A survey of threshold selection techniques," *Computer Graphics Image Processing*, vol. 7, pp. 259–265, 1978.
[4] R. W. Ehich and J. P. Foith, "Representation of random waveforms by relational trees," *IEEE Trans. Comput.*, vol. C-25, pp. 725–736, 1976.
[5] P. V. Sankar and A. Rosenfeld, "Hierarchical representation of waveforms," *IEEE Trans. Pattern Anal. Machine Intell.*, vol. PAMI-1, pp. 73–80, 1979.
[6] J. O. Eklundh and A. Rosenfeld, "Peak detection using difference operators," *IEEE Trans. Pattern Anal. Machine Intell.*, vol. PAMI-1, pp. 317–325, 1979.
[7] D. Rutovitz, "An algorithm for in-line generation of a convex cover," *Computer Graphics Image Processing*, vol. 4, pp. 74–78, 1975.
[8] B. G. Batchelor, "Hierarchical shape description based upon convex hulls of concavities," *J. Cybernetics*, vol. 10, pp. 205–210, 1980.
[9] ——, "Shape descriptions for labeling concavity trees," *J. Cybernetics*, vol. 10, pp. 233–237, 1980.
[10] J. S. Weszka and A. Rosenfeld, "Threshold evaluation techniques," *IEEE Trans. Syst., Man, Cybern.*, vol. SMC-8, pp. 622–629, 1971.
[11] D. L. Milgram, "Region extraction using convergent evidence," *Computer Graphics Image Processing*, vol. 11, pp. 1–12, 1979.

Comments on "Hierarchical Optimization of Nonlinear Dynamical Systems with Nonquadratic Objective Functions"

MARKOS PAPAGEORGIOU

Abstract—**It is shown that the fourth level of a four-level hierarchical optimization algorithm proposed by Fawzy is superfluous.**

In a recent paper[1] Fawzy proposes a four-level hierarchical computation structure for the solution of nonlinear optimization problems of the Mayer form. The original problem considered is given by

$$\min J = \boldsymbol{C}'\boldsymbol{x}(t_f) \tag{1'}$$

subject to

$$\dot{\boldsymbol{x}}(t) = \boldsymbol{f}(\boldsymbol{x}, \boldsymbol{u}, t),$$
$$\boldsymbol{x}(0) = \boldsymbol{x}_0. \tag{2'}$$

In place of (1'), Fawzy introduces a pseudoquadratic functional

$$\bar{J} = \boldsymbol{C}'\boldsymbol{x}(t_f) + \int_0^{t_f}\left[1/2\|\boldsymbol{x}(t)\|_Q^2 + 1/2\|\boldsymbol{u}(t)\|_R^2 + g(\boldsymbol{x}, \boldsymbol{u}, t)\right] dt \tag{3'}$$

with

$$g(\boldsymbol{x}, \boldsymbol{u}, t) = -1/2\|\boldsymbol{x}(t)\|_Q^2 - 1/2\|\boldsymbol{u}(t)\|_R^2$$

and uses some predicted variables $\boldsymbol{x}^*$, $\boldsymbol{u}^*$ to fix g and the nonlinear and interaction terms of $\boldsymbol{f}$.

Selection of the weighting matrices Q, R in (3') might affect the convergence properties of the computation algorithm, but has no influence on the final results, since

$$\boldsymbol{x}^*(t) = \boldsymbol{x}(t) \tag{4'}$$
$$\boldsymbol{u}^*(t) = \boldsymbol{u}(t) \tag{5'}$$

(see (11), (12)) is required in the solution of the optimization problem.

This can also be shown by using the necessary conditions given by Fawzy. The necessary conditions for optimality are given by (11)–(17). Since (16) is equivalent to (18), and on the other hand

Manuscript received February 26, 1982; revised September 10, 1982.
The author is with Dorsch Consult, Ingenieurges, MbH, Postfach 210243, Elsenheimerstrasse 63, 8000 Muenchen 21, Germany
[1]A. S. Fawzy, *IEEE Trans. Syst., Man, Cybern.*, vol. SMC-11, pp. 232–236, Mar. 1981.

0018-9472/83/0300-0235$01.00 ©1983 IEEE